The Shape and Scatter of The Galaxy Main Sequence for Massive Galaxies at Cosmic Noon

arXiv.2105.03766

Sydney Sherman[1*], Shardha Jogee[1], Jonathan Florez[1], Steven L. Finkelstein[1], Robin Ciardullo[2,3], Isak Wold[4], Matthew L. Stevans[1], Lalitwadee Kawinwanichakij[5,6,7], Casey Papovich[6,7], Caryl Gronwall[2,3]

ABSTRACT

We present the main sequence for all galaxies and star-forming galaxies for a sample of 28,469 massive ($M_\star \geq 10^{11} M_\odot$) galaxies at cosmic noon ($1.5 < z < 3.0$), uniformly selected from a 17.5 deg^2 area (0.33 Gpc^3 comoving volume at these redshifts). Our large sample allows for a novel approach to investigating the galaxy main sequence that has not been accessible to previous studies. We measure the main sequence in small mass bins in the SFR-$M_\star$ plane without assuming a functional form for the main sequence. With a large sample of galaxies in each mass bin, we isolate star-forming galaxies by locating the transition between the star-forming and green valley populations in the SFR-$M_\star$ plane. This approach eliminates the need for arbitrarily defined fixed cutoffs when isolating the star-forming galaxy population, which often biases measurements of the scatter around the star-forming galaxy main sequence. We find that the main sequence for all galaxies becomes increasingly flat towards present day at the high-mass end, while the star-forming galaxy main sequence does not. We attribute this difference to the increasing fraction of the collective green valley and quiescent galaxy population from $z = 3.0$ to $z = 1.5$. Additionally, we measure the total scatter around the star-forming galaxy main sequence and find that it is ~ 0.5 – 1.0 dex with little evolution as a function of mass or redshift. We discuss the implications that these results have for pinpointing the physical processes driving massive galaxy evolution.

z~2 星形成銀河をnon-parametricに選択し、Main sequence (MS) を議論

- 宇宙の星形成史のピークであるz~2は(massive) 銀河が星形成を終えてquiescentへ移行し始める時代。
- 銀河のMS (slope, normalization, scatter) は星形成史 (quench, merging) を表すが、MSの評価方法は様々で、何らかの仮定を置くことが多い。
- 大規模サンプルから仮定無しでmain sequenceを定義する手法を確立した。
  - NEWFIRM K_s-selectedカタログ (17.5deg^2@SDSS stripe82, K_s~22.4AB) と多色測光データから28469個 (既存の~40倍) の銀河 (z=1.5—3.0, M_s>$10^{11}M_{sun}$) を抽出。

↓Figure 1. 全サンプルでのM_s-SFR分布。
・Massive endが(Qs,GV増加により) 徐々にflatに。

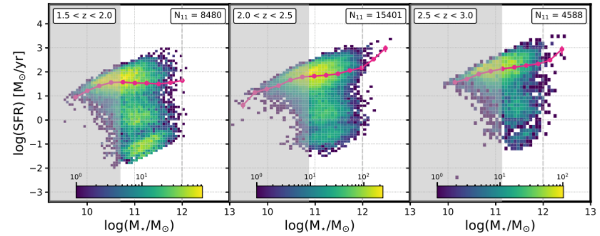

Figure 1. The SFR-M$_\star$ relation (2D histogram) and main sequence (pink circles) for all galaxies in our sample. The main sequence is the average SFR in individual mass bins, while errors on the main sequence are computed using the bootstrap resampling procedure described in Section 3.1. The main sequence for all galaxies shows a flattening at the highest masses ($M_\star = 10^{11}$ to $10^{12} M_\odot$), and this flattening becomes more prominent as time progresses towards $z = 1.5$. Colorbars show the number of galaxies in each cell of the 2D histogram, and gray shaded regions represent masses below our 95% completeness limit. We emphasize that the results presented in this work focus on the mass range $M_\star = 10^{11}$ to $10^{12} M_\odot$, and that results above $M_\star = 10^{12} M_\odot$ (vertical dashed gray line) are unlikely to be robust. Insets on the upper right of each panel show the total number (N_{11}) of galaxies in our sample with $M_\star \geq 10^{11} M_\odot$.

↓Figure 2. SF銀河の抽出。

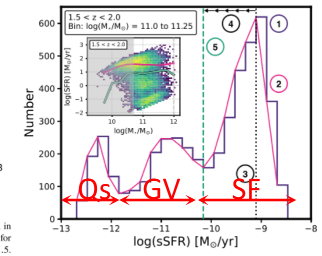

Figure 2. An example schematic of our method used to locate the transition between the star-forming and green valley galaxy populations. The labeled

↓Figure 7. 抽出したSF銀河のM_s-SFR分布 (MS)と分散。
・Massive endのFlat化は見られない➔sSFRがあまり変わっていない。
・分散はMSの下側に偏っている➔従来の対称的なGaussian仮定は×。
Above MSではgas depletion timeが短いというALMA結果とconsistent。

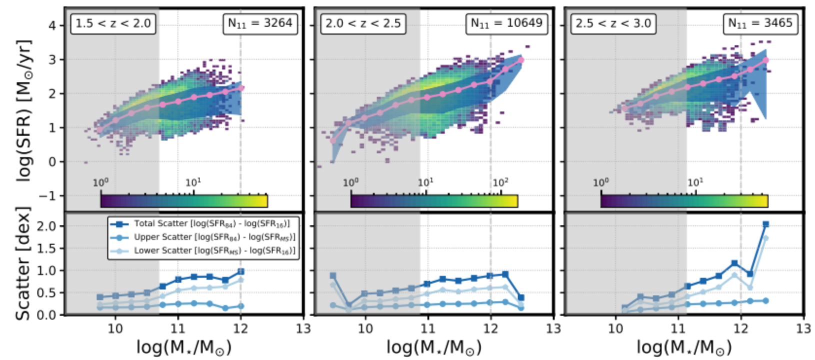

Figure 7. Top Row: The total scatter (blue shaded region) around the star-forming galaxy main sequence (pink) overlaid on the distribution of star-forming galaxies (2D histogram; colorbar indicates the number of galaxies in each 2D bin) in the SFR-$M_\star$ plane. The upper (lower) bound of the blue shaded region is the 84th (16th) percentile of the SFR distribution in a given mass bin. Insets on the upper right of each panel in the top row show the number (N_{11}) of galaxies in the star-forming population in our sample with $M_\star \geq 10^{11} M_\odot$. Bottom Row: The total (squares), upper (circles), and lower (pentagons) observed scatter around the star-forming galaxy main sequence. The total scatter shows a modest increase with increasing stellar mass (less than a factor of three from $M_\star = 10^{11}$ to $10^{12} M_\odot$ in each redshift bin), and the total scatter is fairly constant across our three redshift bins from $z = 1.5$ to $z = 3.0$. In every redshift bin, the lower scatter is larger than the upper scatter by up to a factor of 3. Gray shaded regions represent masses below our 95% completeness limit. We emphasize that the results presented in this work focus on the mass range $M_\star = 10^{11}$ to $10^{12} M_\odot$, and that results above $M_\star = 10^{12} M_\odot$ (vertical dashed gray line) are unlikely to be robust.

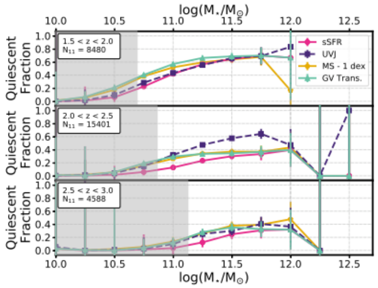

Figure 3. The quiescent fraction as a function of stellar mass determined using the transition between star-forming and green valley galaxies to separate star-forming systems from the collective green valley and quiescent populations (green triangles). Also plotted are the results from Sherman et al. (2020b) who determined the quiescent fraction in three ways: sSFR-selected (pink circles), main sequence - 1 dex selected (gold pentagons), and UVJ-selected (purple squares). The four measurements of the quiescent fraction give consistent results across our three redshift bins spanning $1.5 < z < 3.0$. Gray shaded regions represent masses below our 95% completeness limit. Error bars represent Poisson errors. We emphasize that the results presented in this work focus on the mass range $M_\star = 10^{11}$ to $10^{12} M_\odot$, and that results above $M_\star = 10^{12} M_\odot$ (vertical dashed gray line) are unlikely to be robust. Insets on the upper left of each panel show the total number (N_{11}) of galaxies in our sample with $M_\star \geq 10^{11} M_\odot$.

↑Figure 3. Qs銀河の割合。
・Massiveほど高い ➔ downsizing

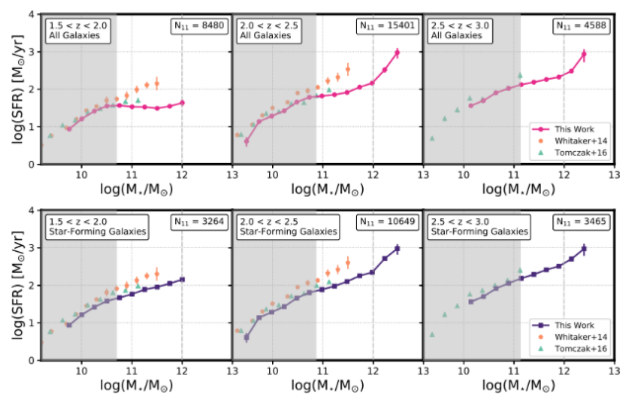

Figure 8. Our empirical main sequence for all galaxies (top row) and star-forming galaxies (bottom row) compared with results from previous observations. We find similar results to those from Tomczak et al. (2016) for both the total (top row) and star-forming (bottom row) galaxy populations. The results from Whitaker et al. (2014) for both the total (top row) and star-forming (bottom row) galaxy populations are higher than our empirical results by a factor of ~ 1.5 – 6.5. Gray shaded regions represent masses below our 95% completeness limit. Insets on the upper right of each panel show the number (N_{11}) of galaxies for the total population (top row) and star-forming population (bottom row) in our sample with $M_\star \geq 10^{11} M_\odot$. We emphasize that the results presented in this work focus on the mass range $M_\star = 10^{11}$ to $10^{12} M_\odot$, and that results above $M_\star = 10^{12} M_\odot$ (vertical dashed gray line) are unlikely to be robust.

↑Figure 8. 他観測結果との比較。

Figure 9. シミュレーションとの比較。→

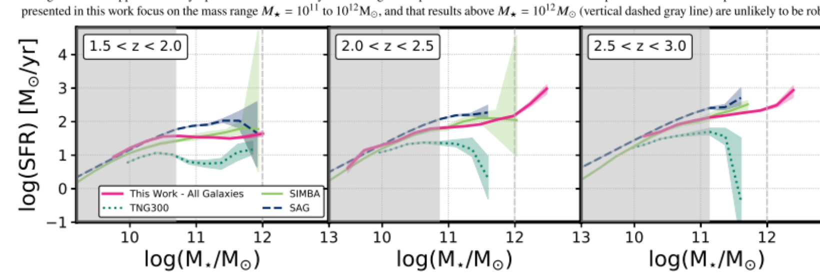

Figure 9. Our empirical main sequence for all galaxies compared with results from hydrodynamical models SIMBA and IllustrisTNG and SAM SAG. The main sequence for all galaxies from SIMBA is within a factor of ~ 1.5 of our empirical result and that from SAG is higher than our empirical result by up to a factor of ~ 3. SIMBA does not show a flattening at the highest masses by $z = 1.5$, while SAG begins to show a flattening high-mass slope towards $z = 1.5$. The main sequence for all galaxies from IllustrisTNG is lower than our empirical result by up to a factor of ~ 10 and shows a strong turnover at the highest masses at $2.0 < z < 3.0$ that is not seen in our empirical result. Gray shaded regions represent masses below our 95% completeness limit. We emphasize that the results presented in this work focus on the mass range $M_\star = 10^{11}$ to $10^{12} M_\odot$, and that results above $M_\star = 10^{12} M_\odot$ (vertical dashed gray line) are unlikely to be robust.

どの計算でもmassive銀河のSFRとflat化とが同時には再現されない。